



Prospects for Solar and Space Weather Research with Polish Part of the LOFAR Telescope

Bartosz P. DĄBROWSKI¹, Andrzej KRANKOWSKI¹,
Leszek BŁASZKIEWICZ^{1,2}, and Hanna ROTHKAEHL³

¹Space Radio-Diagnostics Research Centre, University of Warmia and Mazury, Olsztyn, Poland; e-mail: bartosz.dabrowski@uwm.edu.pl (corresponding author)

²Faculty of Mathematics and Computer Sciences, University of Warmia and Mazury, Olsztyn, Poland; e-mail: leszekb@matman.uwm.edu.pl

³Space Research Centre, Polish Academy of Sciences, Warsaw, Poland; e-mail: hrot@cbk.waw.pl

Abstract

The LOw-Frequency ARray (LOFAR) is a new radio interferometer that consists of an array of stations. Each of them is a phase array of dipole antennas. LOFAR stations are distributed mostly in the Netherlands, but also throughout Europe. In the article we discuss the possibility of using this instrument for solar and space weather studies, as well as ionosphere investigations. We are expecting that in the near future the LOFAR telescope will bring some interesting observations and discoveries in these fields. It will also help to observe solar active events that have a direct influence on the near-Earth space weather.

Key words: telescopes, LOFAR, interferometers, radio, Sun, space weather, ionosphere.

1. INTRODUCTION

The science program of LOFAR is very broad and is organized in “Key Science Projects” (hereafter called KSP). Currently we have the following

KSPs: (i) epoch of reionization, (ii) surveying the low-frequency sky, (iii) the transient radio sky, (iv) pulsar studies and surveys, (v) astroparticle physics, (vi) magnetic fields in the universe, and (vii) solar physics and space weather (van Haarlem *et al.* 2013). The calculations show that LOFAR will be a relevant instrument for Jupiter-like planets with an active moons research. It will be also useful in agriculture field investigations.

In this paper we will focus on solar physics and space weather, as well as ionosphere studies by LOFAR.

2. LOFAR

The LOFAR telescope (www.lofar.org), designed and constructed by ASTRON (the Netherlands Institute for Radio Astronomy), was officially inaugurated by Her Majesty Queen Beatrix in June 2010. It is a large radio interferometer operating in the frequency range 10-240 MHz (corresponding to wavelengths of 30.0-1.2 m). LOFAR consists of an array of dipole antenna stations distributed throughout Europe. Each station contains two antenna fields: LBA (Low Band Antennas) and HBA (High Band Antennas). The LBA occupies an area with a diameter of 80 m (for full configuration – 96 antennas) and operates in the frequency range 10-90 MHz. The HBA antennas occupy an area with a diameter of 62 m (for full configuration – 96 tiles) and operate in the frequency range 110-240 MHz. The lack of receiver in the frequency range 90-110 MHz is a result of using two different front-ends systems (LBA and HBA) and incomparably more electromagnetic interferences (EMI) observed in this radio band. Both LBA and HBA consist of 48 or 96 elements per station. Typical international LOFAR station was presented in Fig. 1.

The total number of LOFAR stations is 50, 38 of which are in the Netherlands and 12 international stations are located in Germany (6 stations), Poland (3 stations), and one station each in France, Sweden, and UK (Fig. 2). Most of the LOFAR stations are located in the Netherlands, 24 of them are parts of the “core”; 6 stations out of that 24 were located on island of about 350 m diameter – “Superterp”. It is situated in the central part of the core. The remaining 14 stations in the Netherlands, called “remote”, are located outside the core at a distance up to 90 km. Each one of the International LOFAR Telescope (ILT) stations is connected by broadband ~10 Gb/s network with data centre in the Netherlands where the correlator is located. When stations are not working in ILT mode, the data from each station can be transferred to local data center (van Haarlem *et al.* 2013).

The angular resolution of the whole LOFAR network depends on the baseline and frequency of observations. For the baseline around 1550 km the angular resolution of the instrument is 0.1 arcsec at 240 MHz (the highest frequency of LOFAR observations) and about 3.2 arcsec at a frequency of

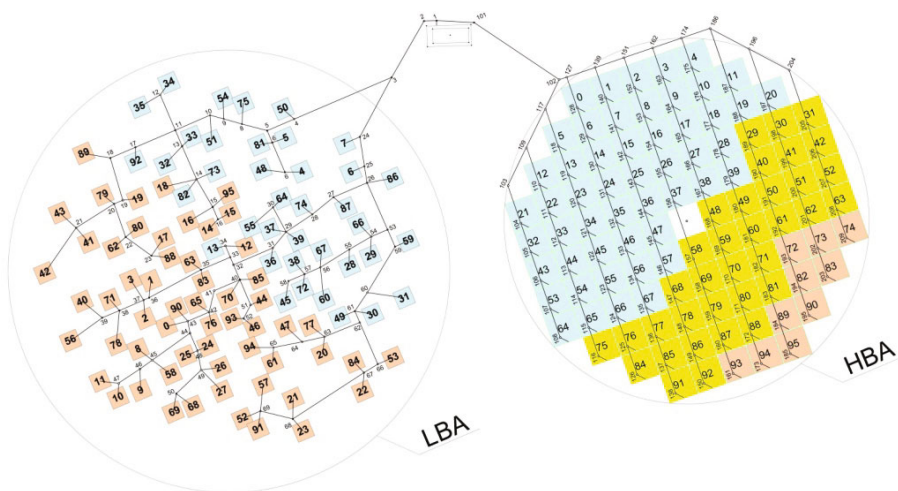


Fig. 1. The configuration of a typical international LOFAR station. The left circle represents the LBA antennas and the right one depicts HBA tiles. Picture taken from ASTRON technical documentation.

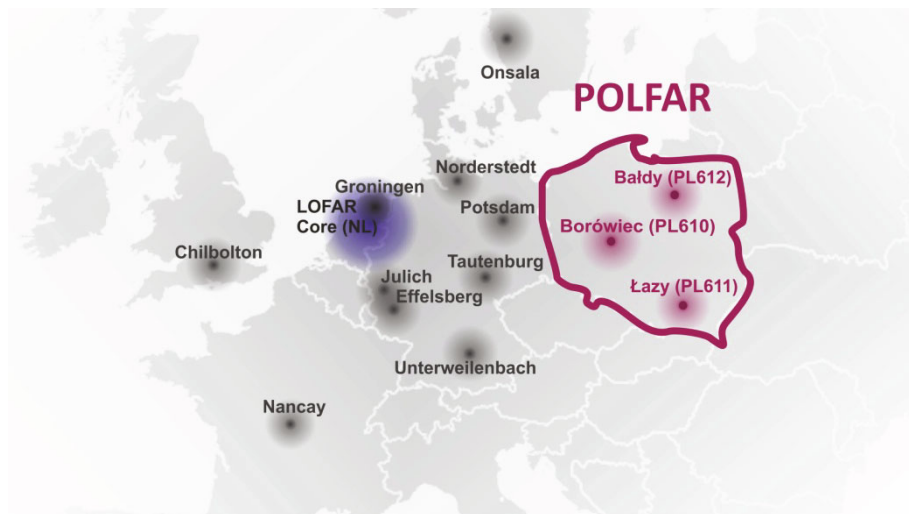


Fig. 2. International LOFAR stations network in Europe. It is formed by 50 stations, of which 38 are in the Netherlands and the rest are scattered across Europe. POLFAR includes three stations: Baldy, Borówiec, and Łazy each of them is marked by a special code (given in parentheses).

10 MHz (the lowest frequency of LOFAR observations). In the case of independent observations, with the use of only three Polish stations (as a separate interferometer), the angular resolution will be around 0.5 arcsec for 240 MHz (Błaszkiwicz *et al.* 2016, van Haarlem *et al.* 2013).

The maximum spectral channel width is 195.3125 kHz, which corresponds to one subband. To provide higher spectral resolution, subband can be split into several channels – usually 16, 64, 256 or 2048. The time resolution is calculated by taking the inverse of the frequency resolution. For typical observations by LOFAR telescope we use 256 channels per subband and we obtain a maximum time resolution of 1.3 ms. For 2048 channels (maximum channels per sub band) we obtain a maximum time resolution of 10 ms (van Haarlem *et al.* 2013).

The expected sensitivity of the LOFAR depends of the array configurations. For the LOFAR core with an 8 hour integration time and an effective bandwidth of 3.66 MHz is 9.0 mJy for 30 MHz and 0.38 mJy for 180 MHz (van Haarlem *et al.* 2013). Some additional information about the technical aspects of LOFAR can be found in Błaszkiwicz *et al.* (2016).

3. POLFAR

POLFAR – Polish LOFAR Consortium – was established in 2007. POLFAR consists of the following institutions: University of Warmia and Mazury (Olsztyn); Jagiellonian University (Kraków); Space Research Center, Polish Academy of Sciences (Warszawa); Szczecin University; Nicolaus Copernicus University (Toruń); Nicolaus Copernicus Astronomical Center, Polish Academy of Sciences (Warszawa); University of Zielona Góra; Wrocław University of Environmental and Life Sciences; and Poznań Supercomputing and Networking Center.

In 2014 a contract for construction of three new LOFAR stations in Poland was signed between ASTRON and POLFAR. These stations were built at Baldy (53°35'45"N, 20°35'26"E, station code: PL612) operated by the University of Warmia and Mazury (Fig. 3), Borówiec (52°16'37"N, 17°04'28"E, station code: PL610), operated by the Space Research Center of the Polish Academy of Sciences, and Łazy (49°57'53"N, 20°29'23"E, station code: PL611) operated by the Jagiellonian University. Such a number of LOFAR stations allows creating an independent interferometer, that can be used when these stations do not take part in the LOFAR network observations. Construction of the three new LOFAR stations in Poland will significantly improve the resolution and sensitivity of the whole LOFAR interferometer. The longest baseline in the LOFAR network is situated between Chilbolton (UK) and Łazy; it is around 1550 km (Krankowski *et al.* 2014).



Fig. 3. The LOFAR station in Baldy (code: PL612).

4. LOFAR AS A TOOL FOR IONOSPHERE STUDY

One of the challenges in the design and operation of the LOFAR telescope is the calibration of the influence of the ionosphere which, at low frequencies, is not uniform and can change within minutes – timescales shorter than the length of observations (Krankowski *et al.* 2007).

At low frequencies (< 300 MHz), at which LOFAR works, the dominant effects of the ionosphere are refraction, propagation delay (Fig. 4) and Faraday rotation. For the LOFAR telescope, the ionosphere is the main source of phase errors in the visibilities (Thompson *et al.* 2001, Intema *et al.* 2009). LOFAR specifications of importance for ionosphere research are presented in Table 1.

Table 1

Specifications of the LOFAR telescope for ionospheric research
(Gaussiran II *et al.* 2004)

Characteristic	LOFAR telescope
Temporal resolution	1 s
Horizontal resolution	2 m
Vertical resolution	2 m
Relative accuracy	< 0.001 TECU (Total Electron Content Units)

The delay per array element depends on the total electron content (TEC) along the line-of-sight through the ionosphere, and therefore on antenna position and viewing direction. The calibration of observations at low fre-

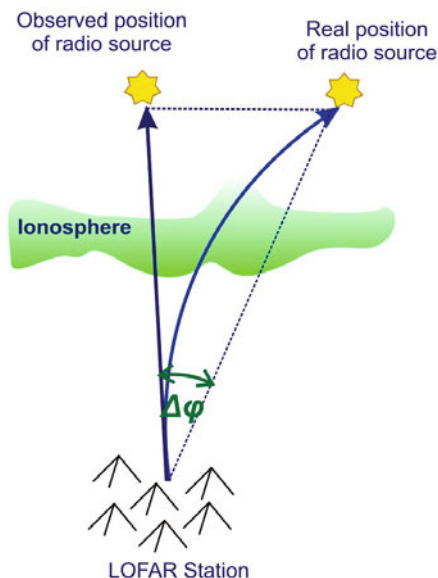


Fig. 4. The ionosphere causes propagation delay differences between array elements, resulting in phase errors ($\Delta\phi$) in the visibilities. The delay per array element depends on the line-of-sight through the ionosphere, and therefore on antenna position and viewing direction. The calibration of observations at low frequencies requires phase corrections that vary over the field-of-view of each antenna (Intema *et al.* 2009).

quencies requires phase corrections that vary over the field-of-view of each antenna (Intema *et al.* 2009). Calibration methods that determine just one phase correction for the full viewing cone of each antenna (like self-calibration) are therefore insufficient. So, special methods of calibration are required and these methods can give us the ionospheric details at the time of observation as an additional result (Sotomayor-Beltran *et al.* 2013).

The calibration methods used in data reduction of the LOFAR network are based on adapting of system to ionospheric conditions. This method is using a known radio source to correct for ionospheric phase distortion on each receiving element of interferometer with the use of ionospheric state predictions. The correction of phase during calibration is just the amendment to the model used and together with the model it is giving the real ionospheric state during observations in source direction for each telescope component. It should also be converted to TEC number and serve in surveys on the structure of the ionosphere (Gaussiran II *et al.* 2004).

The ionosphere changes during the observation within the station beam, and direction-dependent calibration is required (van der Tol and van der

Veen 2007). Also the ionosphere is different for different stations and causes different distortions at different stations. Identifying and removing these radio wave distortions is an excellent opportunity for measurements of the TEC along the line of sight of each LOFAR antenna (Gaussiran II *et al.* 2004).

Currently, most data about the state of the ionosphere comes from the international network of ground-based GPS receivers, operating in real-time. However, the spatial and temporal sampling of available GPS data is not sufficient for complete calibration of radio astronomical measurements and is not reliable enough for ionospheric modeling. However, linking real-time GPS data to the data reduction scheme of telescopes such as LOFAR, as well as linking ionospheric monitoring using known radio sources to tomographic inversion of the ionosphere from GPS measurements, will provide advantages to both disciplines.

Gaussiran II *et al.* (2004) perorate that tomographic techniques can be used to invert the thousands of changing and independent TEC measurements produced by LOFAR into three-dimensional electron density specifications above the array. These specifications will have higher spatial and temporal resolutions than are routinely available by other techniques. These specifications will be used to investigate small-scale changes of ionospheric irregularities, equatorial plasma structures, and ionospheric waves. In addition, LOFAR will improve the understanding of the solar drivers of the ionosphere by simultaneously measuring the solar radio burst and the TEC (Gaussiran II *et al.* 2004).

5. SUN OBSREVATIONS AT METRIC WAVELENGTHS

Solar radio observations are made at a large range of wavelengths. They are divided into microwaves ($f > 3$ GHz), decimeter/meter ($f < 3$ GHz), dekameter ($f < 30$ MHz), and hectometer/kilometer ($f < 3$ MHz) (Warmuth and Mann 2005). All this is also a result of solar radiation properties in different wavelength ranges.

The solar radio emission is a source of information about the structure and dynamics of the solar atmosphere and it can be divided into: (i) quiet Sun component, (ii) slowly varying component, and (iii) sporadic (burst) component (Kundu 1965).

The solar radio burst emission is mainly a plasma emission that is emitted with the local plasma frequency of the source region in corona, or one of its first harmonics. The plasma frequency depends on the electron density and is given by:

$$\nu_p = 8.98 \times 10^3 \sqrt{N_e} \quad [\text{Hz}] ,$$

where N_e is the electron density in cm^{-3} (Melrose 1985). It shows that the emissions on different frequencies come from different layers of the solar atmosphere (the electron density decreases with altitude in the solar atmosphere); the longer the wavelength, the higher the layer where it is formed.

A commonly used coronal density model is the one proposed by Newkirk (1961):

$$N_e(R) = \alpha N_0 \times 10^{4.32 R_s / R}$$

with $N_0 = 4.2 \times 10^4 \text{ cm}^{-3}$, where R is the radial distance from the solar surface (normalized to the solar radius R_s), and the enhancement factor $\alpha = 1 \div 4$ (depending on whether the burst takes place in the quiet corona or near an active region). So the density model of the solar corona provides a link between frequency and height.

If we use the density model of the heliosphere proposed by Mann *et al.* (1999), which is necessary to obtain information about changes in the electron density with the distance from the Sun, then it turns out that the source of radio waves that can be observed by LOFAR, operating in the frequency range 10–240 MHz, are located in the middle and higher corona. At 240 MHz, the highest frequency at which LOFAR operates corresponds to the height $R = 1.17 R_s$. It is also the lowest altitude in the solar atmosphere where we can study radio bursts. It corresponds to approximately 120 000 km above the photosphere. In this region of the solar atmosphere we observe radio burst responding to Coronal Mass Ejections (CMEs). The study of such phenomena is particularly important for space weather because they can trigger ionospheric storms (Mann *et al.* 2007).

6. SOLAR RADIO BURST AT METRIC WAVELENGTHS

In general, we distinguish five main types of solar radio bursts, from type I up to type V (Wild and McCready 1950, Wild 1950a, b). The LOFAR operating in the frequency range 10–240 MHz where can be observe all these events. In this chapter, we will briefly describe each of them. The basic classification of solar radio bursts in the frequency range 25–400 MHz is presented in Fig. 5.

6.1 Type I solar radio bursts

Type I solar radio bursts are narrowband (a few MHz), in general non-drifting and of short duration (< 1 s). This type of bursts appears only at metric wavelengths. They usually occur in large numbers, forming irregular structures superposed on a continuous background. This so-called noise storms can last from a few tens of minutes to several days. Long duration is

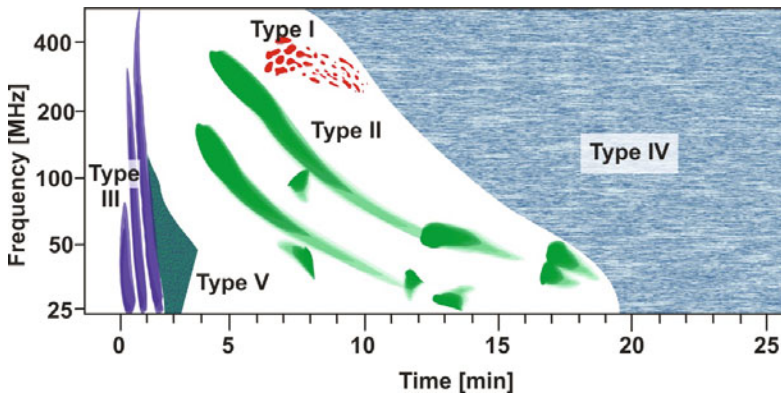


Fig. 5. Schematic diagram shows the basic classification of solar radio bursts in the frequency range 25–400 MHz (based on Ganse *et al.* 2012).

a characteristic feature that distinguishes it from other types of solar radio emission. Their emission mechanism is the fundamental-frequency plasma emission (Melrose 1975).

6.2 Type II solar radio bursts

Type II radio bursts occur in a wide frequency range, from metric to kilometer wavelengths (Nelson and Melrose 1985). This type of bursts is characterized by slowly drifting (rate) from 0.1 up to 1 MHz/s, from high to low frequencies, which means that the exciting agent moves up out of the corona (Warmuth and Mann 2005).

The typical type II bursts show the two-band emission on dynamic spectrum consisting of the fundamental emission band and the harmonic emission band at about twice the frequency of the fundamental one. The fundamental emission refers to the plasma frequency of the emission region, slowly decreasing over time as the coronal/interplanetary shock travels outwards into the heliosphere (Cane *et al.* 1987, Nelson and Melrose 1985). The radio bursts of this type are generated by magneto-hydrodynamic shock waves, which propagate through the solar corona and interplanetary space. In addition, they are associated with flares and CMEs, but there is no one-to-one correspondence.

6.3 Type III solar radio bursts

Particularly important in the study of the processes that occur in solar flares are type III radio bursts. Type III radio bursts have been identified and extracted as a separate class by Wild and McCready (1950). They appear in the range from 1 GHz up to 10 kHz, which corresponds to a source region from

the lower part solar corona up to beyond 1 AU. Type III radio bursts are characterized by high drift rates in frequency (around 100 MHz/s) towards lower frequencies (corresponding to upward movement of the exciting agent in the solar corona) and short duration (seconds). At metric waves the dominant drift is from high to lower frequencies. Type III radio bursts appear in groups, of approximately 10 bursts, and their duration is a few minutes. In the corona, the type III radio emission regions are moving with velocities from about 0.1 to 0.6 c (Benz 2002) with c being the speed of light. Type III radio bursts are caused by the emission of electron beams. These beams are moving up in the solar corona along magnetic field lines stimulating the electron plasma to oscillations with the local plasma frequency (Warmuth and Mann 2005). Acceleration of the electron beam, responsible for generating type III radio bursts, is probable in the areas of magnetic energy release (Aschwanden 2004).

6.4 Type IV solar radio bursts

Type IV radio bursts have been identified for the first time in 1957 by Boischoat and Denisse (1957). Type IV solar radio bursts are broadband continua associated with flares. They are divided into two categories: stationary and moving type IV. The stationary bursts are characterized by a broadband, long lasting continuum with fine structures, like pulsations, zebra patterns, and fiber bursts. They can last from hours to days and they are observed in the range from 20 MHz up to 2 GHz. The moving type IV bursts are characterized by a slow drift in frequency (this corresponds to a movement of the exciting agent with velocities of up to several 100 km/s). The duration of this type of phenomenon is from 30 minutes up to 2 hours and it appears in the range from 20 up to 400 MHz (Warmuth and Mann 2005).

6.5 Type V solar radio bursts

Type V radio events are the rarest type of radio bursts observed. They are broadband continuum emissions that occur generally lower than 200 MHz frequencies. Type V radio bursts start during or right after a group of type III burst, with duration of a minute or so. In the type V model source, coherent Čerenkov plasma waves are excited by fast electrons (speed around $1/3 c$) ejected from a flare and oscillating between mirror points in a magnetic trap in the corona (Weiss and Stewart 1965).

7. SOLAR RESEARCH WITH LOFAR

Solar observations with the LOFAR telescope will be carried out in different basic modes: (i) routine imaging, (ii) solar bursts mode, (iii) joint observation campaigns, and (iv) single stations as spectrometers (Mann 2007). For

observations in these modes we can use a single station or small number of stations. In the following subsections we describe in detail each of these observation modes.

Unfortunately, due to the scattering of radio waves within the solar corona, the spatial resolution of the images is limited to a few 10 arcsec. For this reason, at the beginning it is necessary to use the central core and the nearest remote stations with baseline up to a few 10 km. Once the routine imaging of the Sun is established, it will be possible to investigate to what extent the inclusion of longer baselines does improve the images (Mann 2007).

7.1 Routine imaging

In the routine image Sun monitoring mode, the Sun will be observed at about 20 frequencies through the whole LOFAR band. The images on each of these frequencies should be taken simultaneously. When it comes to the research of the long-term evolution of solar active regions, the proposition is that images would be taken with a cadence of 1/min (Mann 2007).

7.2 Solar bursts model

Solar radio bursts are observed when the LOFAR telescope operates in the burst mode. Solar images will be taken in this mode every 0.1 s, with at least four channels (frequencies) that include frequency pairs separated by a factor of two in order to detect radio radiation on the fundamental and first harmonic frequency. The integration time for a single image will not exceed 50–100 ms. The response time of the LOFAR telescope after observing the flare (*e.g.*, by using another instrument) should be as short as possible, at least less than 1 s. All images on different frequencies should be done at the same time (Mann 2007).

The use of some spectrometer that registers the solar radio bursts at higher frequencies than LOFAR, *e.g.*, up to 800 MHz, is very useful (it corresponds to lower heights in the solar corona). Therefore, in this case it is possible to detect the burst before it reaches the frequency band in which LOFAR works (Mann 2007).

7.3 Joint observation campaigns

Joint observation campaigns with other ground- and space-based instruments, like GREGOR, a solar telescope located at the Observatorio del Teide on Tenerife (visible light and near infrared), Reuven Ramaty High Energy Solar Spectroscopic Imager (RHESSI) satellite (working in X-rays and gamma-rays), NASA's Solar Dynamics Observatory satellite (extreme ultraviolet and visible light), or Atacama Large Millimeter/submillimeter Array (ALMA) radio interferometer (millimetre and submillimetre radio waves)

that observe the Sun in different parts of the electromagnetic spectrum, will let us investigate different aspects of solar activity, like for example solar flares (<http://www.aip.de/groups/osra/sksp/>, access: 16 June 2015).

7.4 Single stations as spectrometers

Using a single LOFAR station, spectroscopic observations of the Sun can be performed. In this case, we obtain a so-called dynamic spectrum which shows the relationship of time, frequency and intensity. It is assumed that in this mode the observations are carried out in all 165 channels, each having a width of 195 kHz. The integration time for each spectrum will be 10 ms. It is estimated that the total time of observations in this mode will be around 8 hours per day. The temporal resolution of such observations must be high enough, so as to be able to observe the solar radio activity phenomenon, whose duration can be several tens of milliseconds (Mann 2007).

8. CONCLUDING REMARKS

On 17 March 2011, during LOFAR's commissioning phase, LOFAR observed a solar radio burst, for the first time. It was a type I radio burst, seen at 150 MHz on the west limb of the Sun (van Haarlem *et al.* 2013).

On 28 February 2013, LOFAR observed, over a period of 30 min, multiple type III radio bursts obtaining radio images as well as high-resolution dynamic radio spectra (Fig. 6). A number of bursts were found to be located at high altitudes, around four solar radii from the solar center in the case of the 30 MHz burst (Morosan *et al.* 2014).

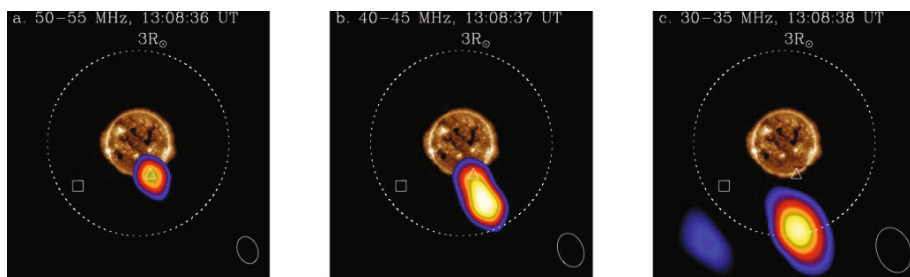


Fig. 6. Images of type III radio burst observed on 28 February 2013 at: (a) 50–55 MHz, (b) 40–45 MHz, and (c) 30–35 MHz, separated by 1 s. On the radio image was superposed the EUV image recorded by the Atmospheric Imaging Assembly onboard NASA's Solar Dynamics Observatory satellite. The triangle and square symbol indicated the location of the beams; for details see Morosan *et al.* (2014). The radius of the dotted white line circle is 3 solar radii. Ellipse marked by a continuous white line, on the lower right corner of each figure, is the telescope beam size. This figure was published in Morosan *et al.* (2014).

The first solar observations with the LOFAR telescope indicate that it is well suited for solar research at low frequencies (from 10 up to 240 MHz). In the near future it will certainly bring some interesting observations and discoveries. It will also help to observe solar active events that have a direct influence on the near-Earth space weather, a good knowledge and prediction of which is of essential importance for our ever increasing dependence on technology from and in space and for the increasing presence of humans in space.

Acknowledgments. The Polish LOFAR stations have been funded by the Polish Ministry of Science and Higher Education; the funds of the large research infrastructure “Construction of the station Polish European LOFAR radio interferometer” (grant No. 6339/IA/158/2013.1).

References

- Aschwanden, M. (2004), *Physics of the Solar Corona. An Introduction*, Springer Verlag, Berlin Heidelberg, 842 pp.
- Benz, A.O. (2002), *Plasma Astrophysics. Kinetic Processes in Solar and Stellar Coronae*, 2nd ed., Kluwer Academic Publ., Dordrecht.
- Błaszkiwicz, L., W. Lewandowski, A. Krankowski, J. Kijak, O. Koralewska, and B. Dąbrowski (2016), Prospects for scrutiny of pulsars with Polish part of LOFAR, *Acta Geophys.* **64**, 1, 293-315, DOI: 10.1515/acgeo-2015-0038.
- Boischot, A., and J.F. Denisse (1957), Les émissions de type IV et l’origine des rayons cosmiques associés aux éruptions chromosphériques, *C. R. Hebd. Acad. Sci. Paris* **245**, 25, 2194-2197 (in French).
- Cane, H.V., N.R. Sheeley Jr., and R.A. Howard (1987), Energetic interplanetary shocks, radio emission, and coronal mass ejections, *J. Geophys. Res.* **92**, A9, 9869-9874, DOI: 10.1029/JA092iA09p09869.
- Ganse, U., P. Kilian, R. Vainio, and F. Spanier (2012), Emission of type II radio bursts – single-beam versus two-beam scenario, *Solar Phys.* **280**, 2, 551-560, DOI: 10.1007/s11207-012-0077-7.
- Gaussiran II, T.L., G.S. Bust, and T.W. Garner (2004), LOFAR as an ionospheric probe, *Planet. Space Sci.* **52**, 15, 1375-1380, DOI: 10.1016/j.pss.2004.09.007.
- Intema, H.T., S. van der Tol, W.D. Cotton, A.S. Cohen, I.M. van Bemmelen, and H.J.A. Röttgering (2009), Ionospheric calibration of low frequency radio interferometric observations using the peeling scheme. I. Method description and first results, *Astron. Astrophys.* **501**, 3, 1185-1205, DOI: 10.1051/0004-6361/200811094.
- Krankowski A., I.I. Shagimuratov, L.W. Baran, and G. Yakimova (2007), The structure of the mid- and high-latitude ionosphere during the November 2004

- storm event obtained from GPS observations, *Acta Geophys.* **55**, 4, 490-508, DOI: 10.2478/s11600-007-0033-3.
- Krankowski, A., L. Błaszkiwicz, K. Otmianowska-Mazur, M. Soida, H. Rothkaehl, and B. Atamaniuk (2014), POLFAR – Polish incarnation of the LOFAR. Scientific objectives and system realization. **In:** *20th Int. Conf. on Microwaves, Radar and Wireless Communications (MIKON)*, 16-18 June 2014, Gdańsk, Poland, DOI: 10.1109/MIKON.2014.6899926.
- Kundu, M.R. (1965), *Solar Radio Astronomy*, John Wiley Interscience Publ., New York.
- Mann, G. (2007), Definition of solar observing modes with LOFAR, Astrophysikalisches Institut Potsdam, http://www.aip.de/groups/osra/documents/Solar_obs_modes.pdf (access: 22 May 2015).
- Mann, G., F. Jansen, R.J. MacDowall, M.L. Kaiser, and R.G. Stone (1999), A heliospheric density model and type III radio bursts, *Astron. Astrophys.* **348**, 2, 614-620.
- Mann, G., C. Vocks, and H. Enke (2007), Solar Physics with LOFAR, Astrophysikalisches Institut Potsdam, <http://www.aip.de/en/research/research-area-cmf/cosmic-magnetic-fields/solar-physics/solar-radio-physics/lofar/solar-physics-with-lofar> (access: 22 May 2015).
- Melrose, D.B. (1975), Plasma emission due to isotropic fast electrons, and types I, II, and V solar radio bursts, *Solar Phys.* **43**, 1, 211-236, DOI: 10.1007/BF00155154.
- Melrose, D.B. (1985), Plasma emission mechanisms. **In:** *Solar Radiophysics: Studies of Emission from the Sun at Metre Wavelengths*, Cambridge University Press, Cambridge, 177-210.
- Morosan, D.E., P.T. Gallagher, P. Zucca, R. Fallows, E.P. Carley, G. Mann, M.M. Bisi, A. Kerdraon, A.A. Konovalenko, A.L. MacKinnon, H.O. Rucker, B. Thidé, J. Magdalenic, C. Vocks, H. Reid, J. Anderson, A. Asgekar, I.M. Avruch, M.J. Bentum, G. Bernardi, P. Best, A. Bonafede, J. Bregman, F. Breitling, J. Broderick, M. Brüggen, H.R. Butcher, B. Ciardi, J.E. Conway, F. de Gasperin, E. de Geus, A. Deller, S. Duscha, J. Eislöffel, D. Engels, H. Falcke, C. Ferrari, W. Frieswijk, M.A. Garrett, J. Griebmeier, A.W. Gunst, T.E. Hassall, J.W.T. Hessels, M. Hoeft, J. Hörandel, A. Horneffer, M. Iacobelli, E. Jette, A. Karastergiou, V.I. Kondratiev, M. Kramer, M. Kuniyoshi, G. Kuper, P. Maat, S. Markoff, J.P. McKean, D.D. Mulcahy, H. Munk, A. Nelles, M.J. Norden, E. Orru, H. Paas, M. Pandey-Pommier, V.N. Pandey, G. Pietka, R. Pizzo, A.G. Polatidis, W. Reich, H. Röttgering, A.M.M. Scaife, D. Schwarz, M. Serylak, O. Smirnov, B.W. Stappers, A. Stewart, M. Tagger, Y. Tang, C. Tasse, S. Thoudam, C. Toribio, R. Vermeulen, R.J. van Weeren, O. Wucknitz, S. Yatawatta, and P. Zarka (2014), LOFAR tied-array imaging of type III solar radio bursts, *Astron. Astrophys.* **568**, A67, DOI: 10.1051/0004-6361/201423936.

- Nelson, G.J., and D.B. Melrose (1985), Type II bursts. **In:** *Solar Radiophysics: Studies of Emission from the Sun at Metre Wavelengths*, Cambridge University Press, Cambridge, 333-359.
- Newkirk, G., Jr. (1961), The solar corona in active regions and the thermal origin of the slowly varying component of solar radio radiation, *Astrophys. J.* **133**, 3, 983-1013, DOI: 10.1086/147104.
- Sotomayor-Beltran, C., C. Sobey, J.W.T. Hessels, G. de Bruyn, A. Noutsos, A. Alexov, J. Anderson, A. Asgekar, I.M. Avruch, R. Beck, M.E. Bell, M.R. Bell, M.J. Bentum, G. Bernardi, P. Best, L. Birzan, A. Bonafede, F. Breitling, J. Broderick, W.N. Brouw, M. Brüggen, B. Ciardi, F. de Gasperin, R.-J. Dettmar, A. van Duin, S. Duscha, J. Eislöffel, H. Falcke, R.A. Fallows, R. Fender, C. Ferrari, W. Frieswijk, M.A. Garrett, J. Grießmeier, T. Grit, A.W. Gunst, T.E. Hassall, G. Heald, M. Hoeft, A. Horneffer, M. Iacobelli, E. Jette, A. Karastergiou, E. Keane, J. Kohler, M. Kramer, V.I. Kondratiev, L.V.E. Koopmans, M. Kuniyoshi, G. Kuper, J. van Leeuwen, P. Maat, G. Macario, S. Markoff, J.P. McKean, D.D. Mulcahy, H. Munk, H. Orru, H. Paas, M. Pandey-Pommier, M. Pilia, R. Pizzo, A.G. Polatidis, W. Reich, H. Röttgering, M. Serylak, J. Sluman, B.W. Stappers, M. Tagger, Y. Tang, C. Tasse, S. ter Veen, R. Vermeulen, R.J. van Weeren, R.A.M.J. Wijers, S.J. Wijnholds, M.W. Wise, O. Wucknitz, S. Yatawatta, and P. Zarka (2013), Calibrating high-precision Faraday rotation measurements for LOFAR and the next generation of low-frequency radio telescopes, *Astron. Astrophys.* **552**, A58, DOI: 10.1051/0004-6361/201220728.
- Thompson, A.R., J.M. Moran, and G.W. Swenson Jr. (2001), *Interferometry and Synthesis in Radio Astronomy*, 2nd ed., John Wiley, New York, 715 pp.
- van der Tol, S., and A.J. van der Veen (2007), Ionospheric calibration for the LOFAR radiotelescope. **In:** *2007 Int. Symp. on Signals, Circuits and Systems, ISSCS (Vol. 2), 13-14 July 2007, Iasi, Romania*, DOI: 10.1109/ISSCS.2007.4292761.
- van Haarlem, M.P., M.W. Wise, A.W. Gunst, G. Heald, J.P. McKean, J.W.T. Hessels, A.G. de Bruyn, R. Nijboer, J. Swinbank, R. Fallows, M. Brentjens, A. Nelles, R. Beck, H. Falcke, R. Fender, J. Hörandel, L.V.E. Koopmans, G. Mann, G. Miley, H. Röttgering, B.W. Stappers, R.A.M.J. Wijers, S. Zaroubi, M. van den Akker, A. Alexov, J. Anderson, K. Anderson, A. van Ardenne, M. Arts, A. Asgekar, I.M. Avruch, F. Batejat, L. Bähren, M.E. Bell, M.R. Bell, I. van Bemmelen, P. Bennema, M.J. Bentum, G. Bernardi, P. Best, L. Birzan, A. Bonafede, A.-J. Boonstra, R. Braun, J. Bregman, F. Breitling, R.H. van de Brink, J. Broderick, P.C. Broekema, W.N. Brouw, M. Brüggen, H.R. Butcher, W. van Cappellen, B. Ciardi, T. Coenen, J. Conway, A. Coolen, A. Corstanje, S. Damstra, O. Davies, A.T. Deller, R.-J. Dettmar, G. van Diepen, K. Dijkstra, P. Donker, A. Doorduyn, J. Dromer, M. Drost, A. van Duin, J. Eislöffel, J. van Enst, C. Ferrari, W. Frieswijk, H. Gankema, M.A. Garrett, F. de Gasperin,

- M. Gerbers, E. de Geus, J.-M. Grießmeier, T. Grit, P. Gruppen, J.P. Hamaker, T. Hassall, M. Hoeft, H.A. Holties, A. Horneffer, A. van der Horst, A. van Houwelingen, A. Huijgen, M. Iacobelli, H. Intema, N. Jackson, V. Jelic, A. de Jong, E. Juette, D. Kant, A. Karastergiou, A. Koers, H. Kollen, V.I. Kondratiev, E. Kooistra, Y. Koopman, A. Koster, M. Kuniyoshi, M. Kramer, G. Kuper, P. Lambropoulos, C. Law, J. van Leeuwen, J. Lemaitre, M. Loose, P. Maat, G. Macario, S. Markoff, J. Masters, R.A. McFadden, D. McKay-Bukowski, H. Meijering, H. Meulman, M. Mevius, E. Middelberg, R. Millenaar, J.C.A. Miller-Jones, R.N. Mohan, J.D. Mol, J. Morawietz, R. Morganti, D.D. Mulcahy, E. Mulder, H. Munk, L. Nieuwenhuis, R. van Nieuwpoort, J.E. Noordam, M. Norden, A. Noutsos, A.R. Offringa, H. Olofsson, A. Omar, E. Orrú, R. Overeem, H. Paas, M. Pandey-Pommier, V.N. Pandey, R. Pizzo, A. Polatidis, D. Rafferty, S. Rawlings, W. Reich, J.-P. de Reijer, J. Reitsma, G.A. Renting, P. Riemers, E. Rol, J.W. Romein, J. Roosjen, M. Ruiter, A. Scaife, K. van der Schaaf, B. Scheers, P. Schellart, A. Schoenmakers, G. Schoonderbeek, M. Serylak, A. Shulevski, J. Sluman, O. Smirnov, C. Sobey, H. Spreuw, M. Steinmetz, C.G.M. Sterks, H.-J. Stiepel, K. Stuurwold, M. Tagger, Y. Tang, C. Tasse, I. Thomas, S. Thoudam, M.C. Toribio, B. van der Tol, O. Usov, M. van Veelen, A.-J. van der Veen, S. ter Veen, J.P.W. Verbiest, R. Vermeulen, N. Vermaas, C. Vocks, C. Vogt, M. de Vos, E. van der Wal, R. van Weeren, H. Weggemans, P. Weltevrede, S. White, S.J. Wijnholds, T. Wilhelmsson, O. Wucknitz, S. Yatawatta, P. Zarka, A. Zensus, and J. van Zwieten (2013), LOFAR: The LOw-Frequency ARray, *Astron. Astrophys.* **556**, A2, DOI: 10.1051/0004-6361/201220873.
- Warmuth, A., and G. Mann (2005), The application of radio diagnostics to the study of the solar drivers of space weather, *Lect. Notes Phys.* **656**, 51-70.
- Weiss, L.A.A., and R.T. Stewart (1965), Solar radio bursts of spectral type V, *Aust. J. Phys.* **18**, 2, 143-166, DOI: 10.1071/PH650143.
- Wild, J.P. (1950a), Observations of the spectrum of high-intensity solar radiation at metre wavelengths. II. Outbursts, *Aust. J. Sci. Res. A* **3**, 3, 399-408, DOI: 10.1071/CH9500399.
- Wild, J.P. (1950b), Observations of the spectrum of high-intensity solar radiation at metre wavelengths. III. Isolated bursts, *Aust. J. Sci. Res. A* **3**, 4, 541-557, DOI: 10.1071/CH9500541.
- Wild, J.P., and L.L. McCready (1950), Observations of the spectrum of high-intensity solar radiation at metre wavelengths. I. The apparatus and spectral types of solar burst observed, *Aust. J. Sci. Res. A* **3**, 3, 387-398, DOI: 10.1071/CH9500387.

Received 19 October 2015

Received in revised form 17 February 2016

Accepted 19 April 2016